Structural Design of Robust and Biocompatible Photonic Hydrogels from an In Situ Cross-Linked Hyperbranched Polymer System

Zhang, Jing; Yong, Haiyang; A, Sigen; Xu, Qian; Lyu, Jing; Gao, Yongsheng; Zeng, Ming; Zhou, Dezhong; Yu, Ziyi; Tai, Hongyun; Wang, Wenxin

Chemistry of Materials

DOI:
10.1021/acs.chemmater.8b02542

Published: 11/09/2018

Peer reviewed version

Structural design of robust and biocompatible photonic hydrogels from an *in-situ* crosslinked hyperbranched polymer system

Jing Zhang,[†] Haiyang Yong,[†,‡] Sigen A,[†] Qian Xu,[†] Yongpeng Miao,[†,‡] Jing Lyu,[†] Yongsheng Gao,[†] Ming Zeng,[†] Dezhong Zhou,[†]* Ziyi Yu,[§] Hongyun Tai,[∥] and Wenxin Wang[†]*

[†]Charles Institute of Dermatology, School of Medicine, University College Dublin, Dublin 4, Ireland.

[‡]School of Materials Science and Engineering, Tianjin University, Tianjin 300072, China.

[§]Department of Chemistry, University of Cambridge, Lensfield Road, Cambridge CB2 1EW, UK.

[∥]School of Chemistry, Bangor University, Bangor, Gwynedd LL57 2DG, UK.

ABSTRACT: Multifunctional hyperbranched poly(poly(ethylene glycol) diacrylate) (HB-PEGDA) polymers with well-defined composition, structure and functionality are proposed in this work as photonic hydrogel scaffolds. By taking advantage of its unique transparency, low intrinsic viscosity and high amount of vinyl groups, the HB-PEGDA can effectively penetrate inside the colloidal photonic crystal (CPC) substrate and be crosslinked with thiolated hyaluronic acid very quickly. This photonic hydrogel shows not only an unexpected protective effect to the untreated CPC substrate, but also non-swelling characteristics attributed to its relatively compacted network structure, which leads to robust structural integrity and credible, consistent optical performance under complex physiological conditions. Moreover, this photonic hydrogel shows good biocompatibility and can be easily modified to introduce specific functions (*e.g.*, cell attachment), providing novel insights into the photonic hydrogel design towards diverse bio-optical applications.

INTRODUCTION

Colorimetric materials have been widely applied in the areas ranging from chemical sensing,[1–5] clinical diagnostics,[6,7] to food industry[8] and information storage.[9] Their "readout" colours are normally determined by the aggregation state of nanoparticles,[10–12] structural change of organic dyes[13] or catalysis of enzymes,[14] *etc*. In the past few decades, structural colours arising from the interaction of light with photonic nanostructures have aroused great interests.[15-17] In comparison with other types of colouring, the structural coloration has obvious advantages: it is free from photochemical degradation; the colours are purer due to the comparable length scale between nanostructure spacing and reflectance wavelength of the light;[18] and more significantly, it enables the anti-interference of colorimetric detection.[19–21]

Up to date, a variety of strategies including layer-by-layer manufacture,[22] semiconductor fabrication,[23] holographic lithography,[24] and self-assembly[25–27] have been developed to achieve such structural colours. Among them, monodispersed colloidal particles undergoing self-assembly into an ordered array of colloidal photonic crystal (CPC) is one of the simplest and least inexpensive methods. However, the deterioration and accumulation of damage of the CPCs during direct uses would cause severe colour loss,[28] sample contamination, or even high cytotoxicity in biological applications.[29] Hence, in practice, in order to increase their survivability, CPCs are normally embedded into diverse hydrogel scaffolds or transformed into inverted opals to form a photonic hydrogel. For instance, Asher *et al.* fixed susceptible crystalline colloidal arrays (CCA) within the stimuli-sensitive polyacrylamides to achieve tunable diffracting arrays.[30] Ge's group proposed the immobilisation of polycrystalline SiO_2 colloidal film into the photo-polymerized poly(ethylene glycol)s (PEGs).[31] Zhang and *co*-workers introduced the strong polyelectrolytes into the photonic hydrogel design to enhance the interference-resistant performance.[32] Very recently, Gu *et al.* demonstrated the use of methacrylated gelatin (GelMA) to prepare inverse opal-structured photonic hydrogel, mimicking natural organisms.[33] On one hand, due to the high sensitivity of these photonic hydrogels to the external stimuli, diverse sensing devices have been successfully designed with response to changes in ionic strength,[20] pH,[34,35] light,[36,37] mechanical stress,[38] temperature[39] or magnetic field.[40] On the other hand, however, the high susceptivity of photonic hydrogels causes major challenges for applications in the areas such as bar-coding and information storage where credible, consistent structural colours are generally required. Additionally, its biocompatibility together with tunable elastic properties is another major concern especially for bio-related uses, as they play important roles in diverse cell processes like growth, division, migration, differentiation, *etc*. However, unfortunately, up to date almost all the photonic hydrogels are fabricated through the free radical polymerization of monomers, which re-

sults in: 1) easy dissolve of the pre-formed polycrystalline colloidal films; 2) slow gelation process; 3) residual monomers which are not biocompatible; 4) difficulty in modification of the hydrogels. From this perspective of view, utilization of hyperbranched polymers (HBPs), instead of monomers, to fabricate photonic hydrogels would have unique advantages: 1) HBPs have relatively lower solubility to the pre-formed polycrystalline colloidal films; 2) can be crosslinked to form hydrogels more quickly; 3) have no residual monomers and therefore higher biocompatibility.

HBPs are a type of dendritic polymers displaying a three dimensional (3D) structure with multiple terminal groups, which afford them with a series of attractive features for diverse applications.[41-43] Of all the HBPs, the ones prepared from controlled (*co*)polymerization of multivinyl monomers (MVMs) have attracted significant attentions because: 1) the wide availability of MVMs and great advances in the controlled/living polymerization methods make the composition, structure and functionality of the resulting HBPs highly tunable; 2) there are multiple pendant vinyl groups in the HBPs which can be used for functionalization through a variety of chemistries such as photochemistry, thiol-ene Michael addition *etc*. By kinetically controlled polymerization of MVMs, our group has successfully prepared a series of HBPs with high branching degree (BD) and pendent vinyl group content *via* the deactivation enhanced atom transfer radical polymerization (DE-ATRP)[44-46] and reversible addition-fragmentation chain transfer polymerization (RAFT).[47] These HBPs have been used in gene delivery,[48] injectable tissue engineering scaffolds[49] and wound adhesives[50] *etc*.

Recently, using the tetraethylthiuram disulfide (DS), a 60 years old FDA-approved anti-cancer drug, as the RAFT agent precursor, we have developed an *in-situ* RAFT polymerization strategy: RAFT agent is generated *in-situ* from the precursor to control the polymerization.[51] Utilizing this new approach, poly(ethylene glycol) methyl ether acrylate (PEGMEA), poly(methyl methacrylate) (PMMA) and poly(butyl acrylate) (PBA) with well-defined structure were synthesized. What should be noted is that the polymers synthesized from the *in-situ* RAFT polymerization are colourless, which would be of extra advantage for their application in optical areas. We can envisage that the *in-situ* RAFT polymerization can, in principal, be used to prepare HBPs from MVMs for fabrication of photonic hydrogels.

In this work, we propose the utilization of HBPs to prepare novel photonic hydrogels and demonstrate their unique properties. A hyperbranched poly(poly(ethylene glycol) diacrylate) (HB-PEGDA) was synthesized by the *in-situ* RAFT polymerization using DS as the RAFT agent precursor (**Figure 1a**). Due to its good transparency, low viscosity and high content of vinyl groups, the HB-PEGDA can penetrate the CPC substrate easily and be crosslinked with thiolated hyaluronic acid (HA-SH, see structure in **Figure S1**) to form photonic hydrogel quickly. Importantly, the whole impregnation process does not induce significant destruction to the CPC internal structure; the compacted network structure of the HB-PEGDA maintains the structural integrity of the photonic hydrogel very well, even under complex physiological conditions. Moreover, benefited from the non-immunogenic and bio-inert poly(ethylene glycol) (PEG) and hyaluronic acid (HA), a linear glycosaminogly derived from the natural extracellular matrix (ECM), the photonic hydrogel exhibits excellent biocompatibility. In addition, functional moieties (*e.g.*, cell adhesion molecules, CAMs) can be further introduced to the photonic hydrogels to enhance its function for specific applications.

RESULTS AND DISCUSSION

2.1. Synthesis of HB-PEGDA via the *in-situ* RAFT homopolymerization of MVMs

The DS mediated *in-situ* RAFT strategy can successfully control the polymerization of monovinyl monomers. However, its feasibility for MVMs has not been explored yet. Using DS as the RAFT agent precursor, 2'-azobis(2-methylpronitrile) (AIBN) as the initiator, the homopolymerization of PEGDA (average M_n= 700) (0.4 mol·L^{-1}) was carried out in butanone at 70 °C with a feed ratio of [PEGDA] : [DS] : [AIBN] at 25 : 1 : 1.4. Gel permeation chromatography (GPC) was used to monitor the evolution of polymer molecular weight during the polymerization. As shown in **Figure 1b** and **Table S1**, at the very beginning, the polymer molecular weight increased steadily with time and showed a unimodal peak with the *Đ* remained <1.5, which suggested that polymer chain propagation dominated at this stage because the high concentration of unreacted monomers favours the generation of linear polymeric chains with pendant vinyl groups.[52] As the reaction proceeded, significant levels of the monomer have been consumed, the propagation centers tend to react with the pendent vinyl groups on other chains, which led to intermolecular combination generating hyperbranched structures and thus dramatically increased molecular weights and broad *Đ* were observed.[44,53] The recorded plots showed that the polymerization followed first order kinetics and concentration of the propagation centers remained almost unchanged (**Figure 1c**), demonstrating the good control of the polymerization mediated by the *in-situ* formed RAFT agent from DS and AIBN.[51]

To obtain HB-PEGDA with moderate molecular weight, the polymerization was stopped at 40% monomer conversion. The polymers were purified by precipitation and the chemical structures were confirmed by NMR (**Figure S2-S4**). The branching ratios of the HB-PEGDA were calculated to be around 30%, indicating around 70% of the pendant vinyl ratios were remained (**Figure S3**), which would provide multiple reaction sites for further modification. Mark-Houwink plot alpha values (α) of the representative HB-PEGDA were 0.26 and 0.18 (**Figure 1d**), respectively, further demonstrating their highly branched structures. The HB-PEGDA polymers were colourless and transparent. UV-*vis* absorption spectra showed that

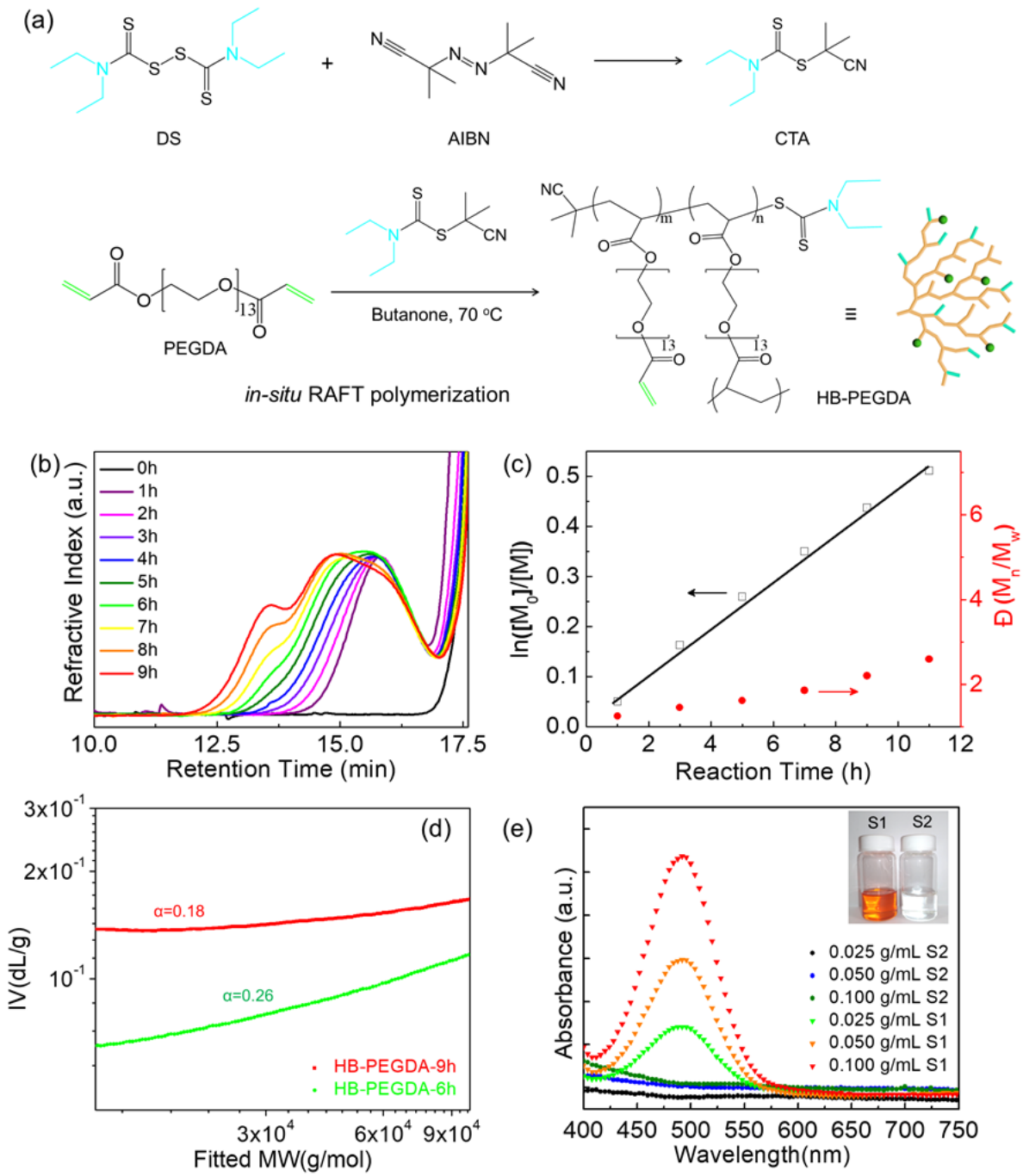

Figure 1. a) Synthesis of HB-PEGDA via an *in-situ* RAFT polymerization. The RAFT agent was formed in-situ from the initiator AIBN and DS. b) GPC traces of HB-PEGDA polymers isolated at different polymerization time; c) Plots of $\ln([M_0]/[M])$ and molecular weight distribution ($Đ$) *versus* polymerization time; d) Mark-Houwink plots of the HB-PEGDA polymers isolated at the polymerization time of 6 and 9 hours, respectively; e) UV-*vis* spectra of the HB-PEGDA polymers synthesized with CPDB (Sample S1) as the RAFT agent and DS as the RAFT agent precursor (Sample S2). The inset photo corresponds to their optical images.

there was no obvious absorption in the visible region (labelled as Sample S2 in the inset of **Figure 1e**). In contrast, HB- PEGDA (labelled as Sample S1) prepared using the conventional RAFT agent 2-cyanoprop-2-yl dithiobenzoate (CPDB) had a strong absorption peak at the wavelength of 480 nm derived from the CPDB residues. These results highlighted the potential applications of the HB-PEGDA synthesized from the *in-situ* RAFT polymerization in optical areas.

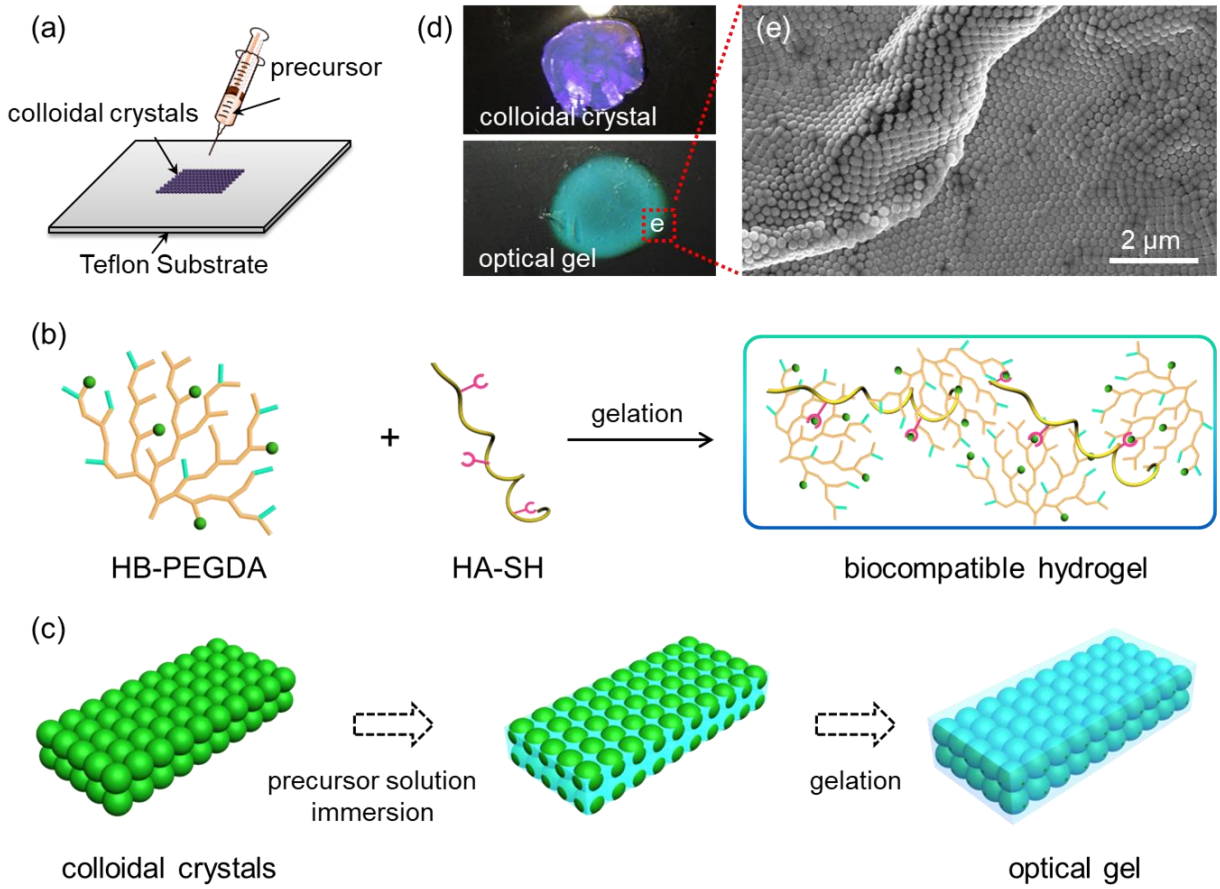

Figure 2. Schematic illustration of a) the preparation process of the HB-PEGDA/HA-SH hydrogel-CPC composite; b) The formation of the injectable hydrogels *via* the thiol-ene Michael addition chemistry; c) Encapsulation of the CPC with the injectable HB-PEGDA/HA-SH pregel; d) The optical images of the CPC before and after HB-PEGDA/HA-SH hydrogel impregnation; e) SEM image of the resulting hydrogel-CPC composite. The CPC film was composed of SiO_2 particles with a diameter of 209 nm. The final polymer concentrations for preparing hydrogel-CPC composites are: HB-PEGDA (3%, w/v); HA-SH (0.5%, w/v).

2.2. Construction of hydrogel-CPC composites

In general, the heat pre-treatment is an indispensable step for preparing hydrogel-CPC composites/inverted opals, because a certain mechanical strength is required to avoid colloid peeling or lattice distortion of the CPCs during the impregnation and gel formation steps. There are multiple pendent vinyl groups on the HB-PEGDA, which can be crosslinked to form hydrogels *via* diverse chemistry, such as such as photo-polymerization, thiol-ene Michael addition *etc*. Therefore, we propose to use an injectable hydrogel system composed of the HB-PEGDA and HA-SH to directly encapsulate the untreated CPCs (**Figure S5**). Briefly, the aqueous mixture solution containing 3% (w/v) HB-PEGDA and 0.5% (w/v) HA-SH (Glycosil®, ESI BIO) was transferred onto the untreated CPC film surface (**Figure 2a**), and the gelation occurred spontaneously through the thiol-ene Michael addition reaction (**Figure 2b** and **Figure 2c**).[54] After gelation, a purple to blue-green colour change (**Figure 2d**) could be clearly observed. This is because the air interstices (refractive index = 1) of the CPC film were replaced by the hydrogel components (refractive index = 1.3 - 1.5) (**Figure S6**), leading to an increase of the average refractive indexes and hence the red shift of the diffraction peak. The top-view SEM image (**Figure 2e**) shows the colloid spheres were orderly embedded in the hydrogel with its close-packed plane (1 1 1) oriented parallel to the substrates. These features along with the narrow peak width (**Figure S7**) suggest that the direct impregnation of HB-PEGDA/HA-SH hydrogel into the untreated CPC film does not impose significant destructive effect on either its structure or optical performance.

To decipher the possible mechanism of the non-destructive effect, the gelation process of the HB-PEGDA/HA-SH mixture was studied through oscillation rheology analysis (**Figure 3**). Significantly, a very quick gelation was observed as evidenced by the rapidly increased storage modulus (*G'*). And in general, a higher HB-PEGDA concentration or temperature would substantially speed up the gelation process (**Figure 3a** and **Figure 3b**). Interestingly, the HB-PEGDA/HA-SH ratio has

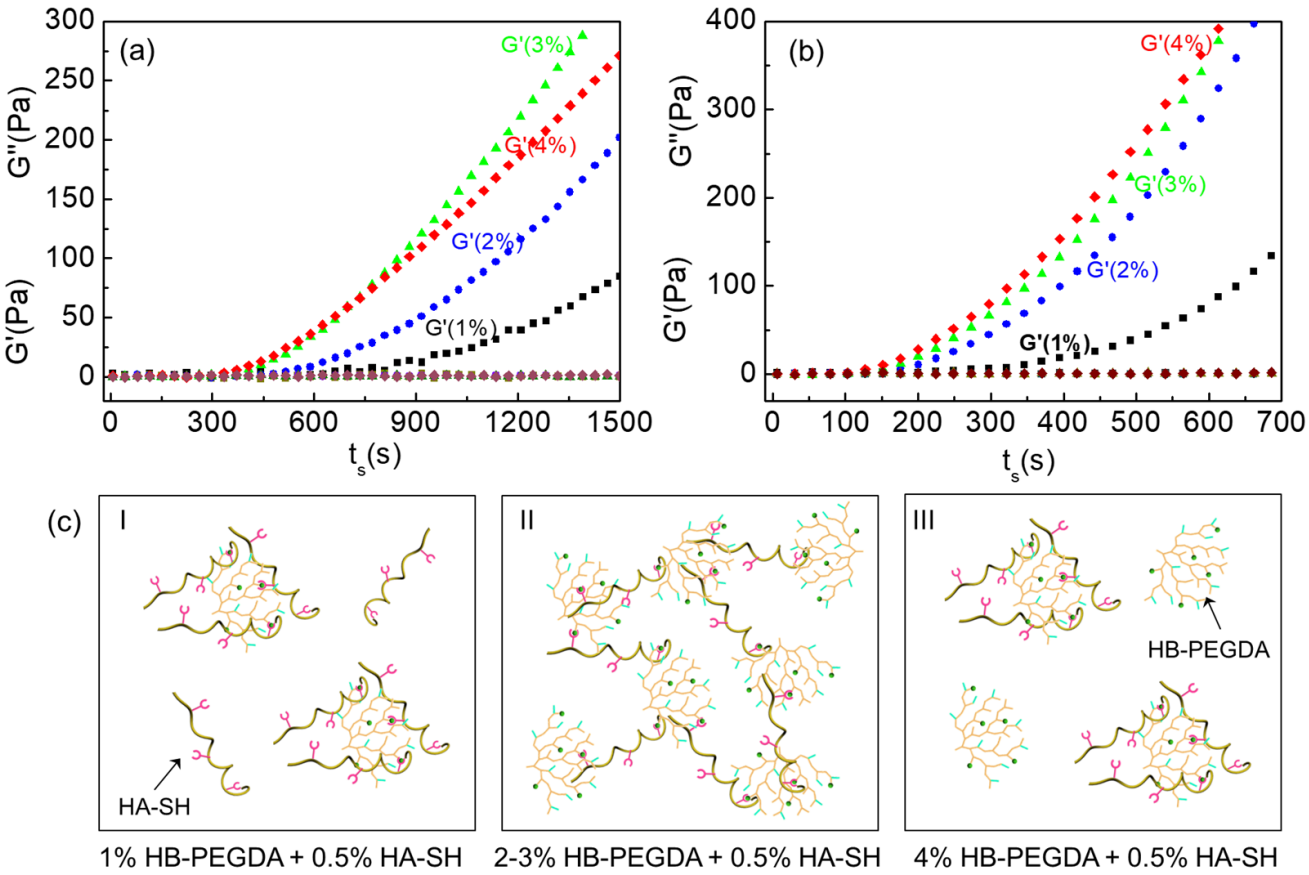

Figure 3. Real time rheological measurements of the HB-PEGDA/HA-SH (0.5% w/v) mixture at a) 20 and b) 37 °C, respectively. Herein, HB-PEGDA polymer concentration varied gradually from 1% (w/v) to 4% (w/v); G' and G'' represent the storage modulus and loss modulus of the forming HB-PEGDA/HA-SH hydrogels, respectively. c) The possible early-stage cross-linking mechanisms of the HB-PEGDA/HA-SH injectable hydrogels with different ratios of HB-PEGDA to HA-SH.

an interesting effect on the *G'* at the early stage of gelation: when a low (*e.g.*, 2:1) or high (*e.g.*, 8:1) ratio was used, a relatively lower *G'* was detected. In contrast, a moderate ratio (*e.g.*, 4:1 and 6:1) led to a relatively higher *G'*. We speculate that when a low or high ratio was used, the less HB-PEGDA (or HA-SH) molecules were surrounded and stabilized by the excess HA-SH (or HB-PEGDA) to form aggregates or microgels (Case I or III in **Figure 3c**). However, since the aggregates or microgels turn into the macroscopic hydrogel very quick, it is thus challenging to conduct extra intuitive measurements, such as DLS, SEM *etc.* to further confirm our hypothesis. In contrast, a moderate ratio lead to formation of macrogels (Case II of **Figure 3c**). All the aggregates, microgels and macrogels were further crosslinked to form the macroscopic hydrogels in minutes. The three-dimensional (3D) and crosslinked network structure of the hydrogel stabilized and protected the crystal films spontaneously. Thus, the possible destruction during impregnation and gelation was omitted. To further confirm this, PEGDA monomer was directly used to fabricate the photonic hydrogels, the crystal films was dissolved and thus destructed immediately when the monomer was dropped onto the films. Furthermore, as **Figure S8** shows, increasing the polymer concentration for hydrogel-CPC composites formation results in a sharp increase of the storage modulus. As the elastic properties of the hydrogel-CPC composites play important roles in a variety of cell processes,[55] this tuneable characteristic is significant for diverse bio-related uses. It should be noted that PEGDA monomer was also directly used to copolymerize with the HA-SH, however, as the rheological measurements show (**Figure S9**), under the same polymer concentration, PEGDA/HA-SH cannot form hydrogels, which may attribute to the low molecular weight and relatively low vinyl group contents.

In addition to the protective effect, the injectable hydrogel also endows the hydrogel-CPC composites with robust optical performance. As shown in **Figure 4a**, over 7 days of incubation in phosphate-buffered saline buffer (PBS, 0.1 M) at 37 °C, the reflection peak of the HB-PEGDA/HA-SH photonic hydrogel remained almost constant, in sharp contrast with that of the conventional hydrogel networks.[56] This could be attributed to the low swelling feature of the HB-PEGDA/HA-SH hydrogel:

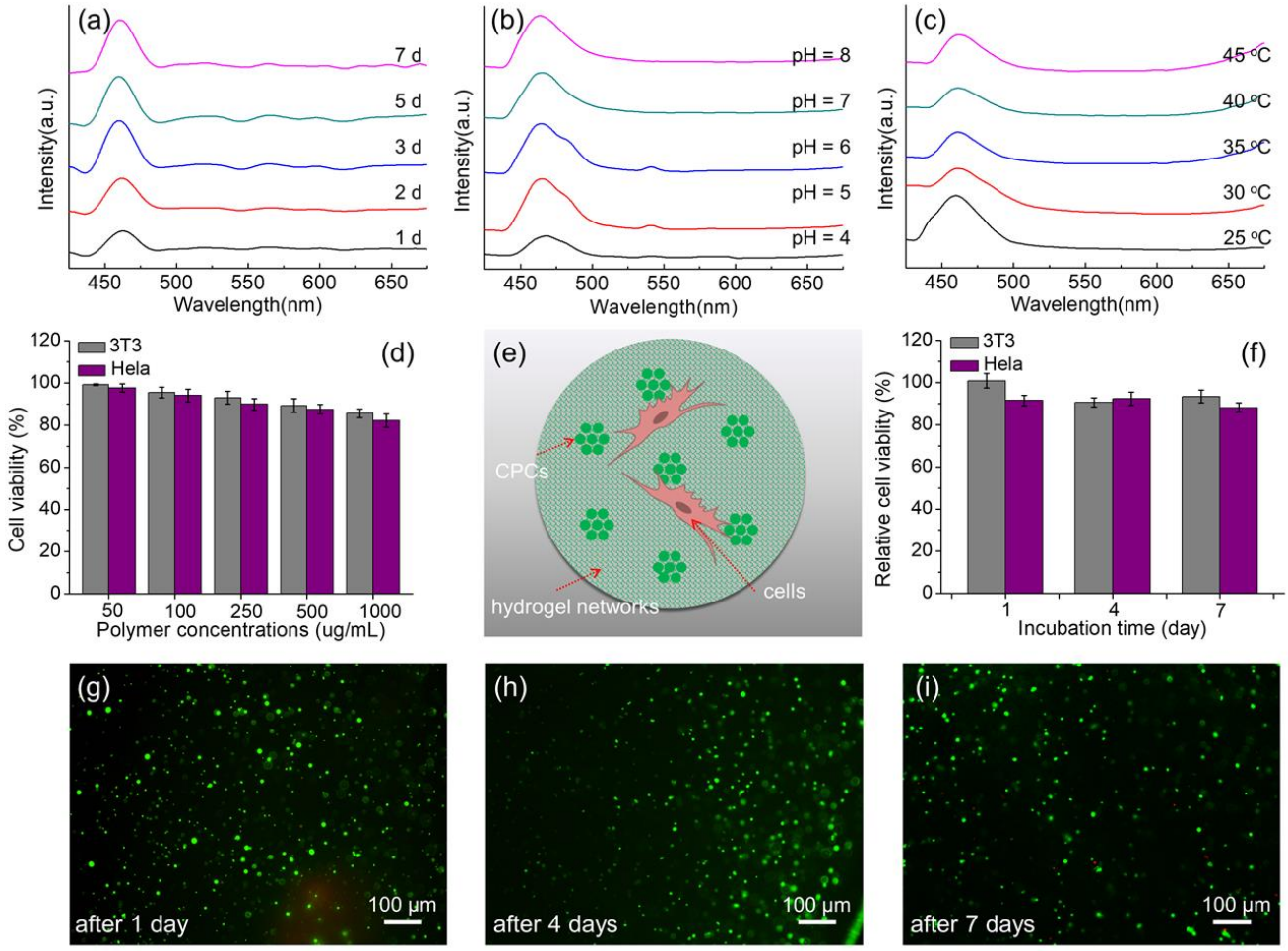

Figure 4. a-c) The reflectance spectra of the HB-PEGDA/HA-SH hydrogel-CPC composite at different swelling time, pH and temperature; d) Percentage of live cells to the total cell number calculated from LIVE/DEAD assay after *co*-culture with the HB-PEGDA polymer of different concentrations; e) Schematic illustration of the formation of HB-PEGDA/HA-SH hydrogel-CPC composite; f) Percentage of live cells (embedded in the hydrogel-CPC composite) to the total cell number calculated from LIVE/DEAD assay and corresponding g-i) representative fluorescence images. Calcein AM (green) stain for live cells and ethidium homnodimer-1 (red) for dead cells. The final polymer concentrations for preparing the hydrogel are: HB-PEGDA (5%, w/v) and HA-SH (1%, w/v).

the HB-PEGDA molecules with high vinyl group content (**>60%, Table S1**) manifest a three-dimensional (3D) structure with a relatively less flexibility in the interior, so when crosslinking by the HA-SH, a high amount of cross-linked junctions were formed, which led the globular HB-PEGDA molecules to bind up with each other closely, generating a very compact network structure with limited swelling ability.[57] Moreover, the HB-PEGDA/HA-SH hydrogel also enabled the composites to maintain a stable colour under various pH and temperature conditions (**Figure 4b** and **Figure 4c**). The credible, consistent colours without any compromise in complex physicochemical conditions are especially appealing for the application of the hydrogel-CPC composites in bioencoding.

2.3. Biocompatibility of the HB-PEGDA/HA-SH photonic hydrogel

PEG and HA based components have been widely demonstrated for their excellent biocompatibility. Cytotoxicity of the HB-PEGDA polymer and HB-PEGDA/HA-SH photonic hydrogel was further evaluated by using LIVE/DEAD® (Molecular Probes®) assays. 3T3 and HeLa cells were incubated with the HB-PEGDA polymer at the concentration ranging from 50 to 1000 μg/mL. As shown in **Figure 4d**, after 24 hours of incubation, for the both cell types, HB-PEGDA did not induce obvious cytotoxicity, even at the concentration of 1000 μg/mL, over 85% cell viability was preserved. The cytotoxicity test for the photonic hydrogel was conducted by mixing the cells into the HB-PEGDA/HA-SH mixture before transferring it onto the CPC surface (**Figure 4e**). As shown in **Figure 4f**, over 80% of the embedded cells were viable in the composites over one week, indicating the high biocompatibility of the

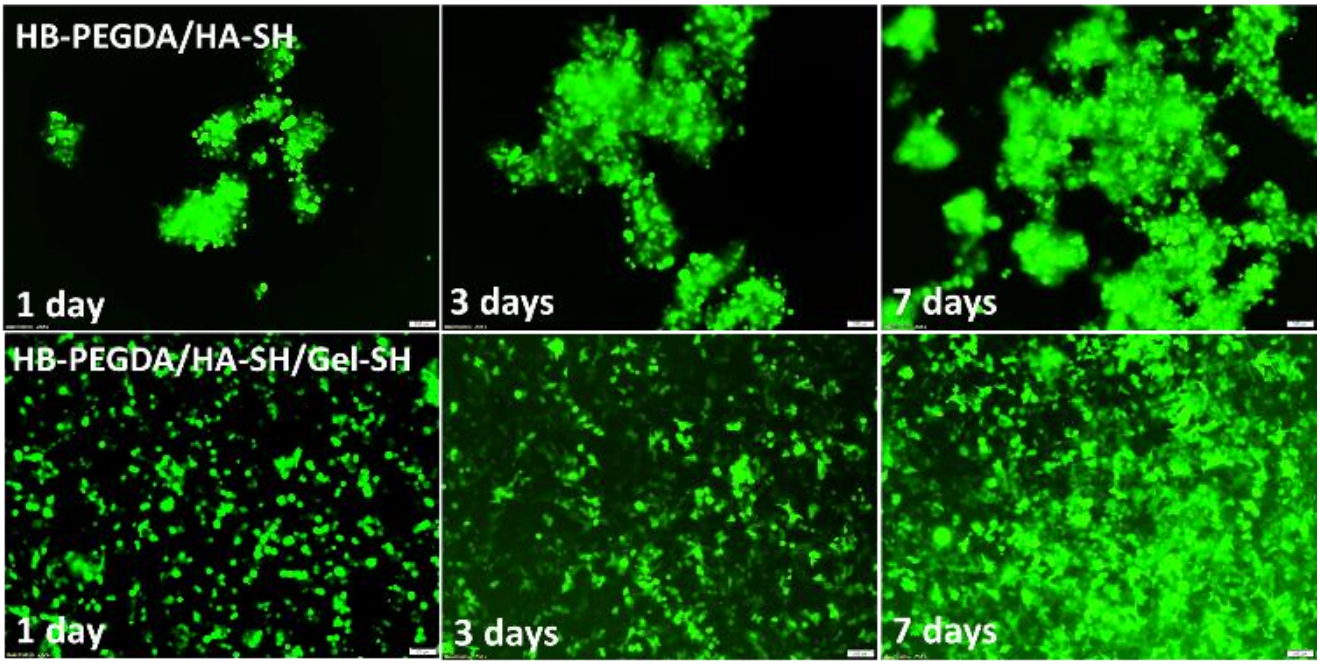

Figure 5. Fluorescent images of the stably green fluorescent protein (GFP) expressing HeLa cells after seeding on top surfaces of two kinds of hydrogel-CPC (HB-PEGDA/HA-SH/CPC and HB-PEGDA/HA-SH/Gel-SH/CPC) composites at day 1, day 3 and day 7. The solution concentrations (w/v) for prepare the hydrogel are: HB-PEDGA, 4%; HA-SH, 1%; Gel-SH, 1%. The scale bars present 200 μm.

hydrogel. The live/dead images further show that only very few dead cells (red) were observed (**Figure 4g-i**). The excellent biocompatibility would make the HB-PEGDA/HA- SH photonic hydrogel more desirable for applications in the fields such as bio-encoding *etc.*

2.4. Functionalization capacity of the HB-PEGDA/HA-SH photonic hydrogel

The multiple pendent vinyl groups impart the HB-PEGDA/HA-SH photonic hydrogel multiple reaction sites for functionalization. Theoretically, diverse functional components can be introduced into the photonic hydrogel through thiol-ene click chemistry or radical chemistry *etc*. Cell attachment capacity is a significant aspect to achieve cells-on-optical barcode platforms for bioencoding applications. To improve the cell attachment capacity, several cell adhesion molecules (CAMs) such as arginyl-glycylaspartic acid (RGD) peptide, and full-length proteins including collagen, fibronectin, *etc.* were introduced into the photonic hydrogels. However, due to the relatively large hydrogel pore sizes, complex physical or chemical bonding was usually required for efficient CAM encapsulation. As a proof-of-concept, here we introduced gelatin - a type of CAM that has been wide used to enhance cell attachment to our HB-PEGDA/HA-SH photonic hydrogel. By simply mixing the thiolated gelatin (Gel-SH), HA-SH and HB-PEGDA together and then transferred onto the CPC surfaces, the thiol groups in both Gel-SH and HA-SH reacted with the vinyl groups on the HB-PEGDA simultaneously and a HB-PEGDA/HA-SH/Gel-SH photonic hydrogel was prepared. Cell attachment studies showed that with the introduction of gelatin, the cell attachment ability of the photonic hydrogel was substantially enhanced. As shown in **Figure 5**, on the HB-PEGDA/HA-SH/CPC hydrogel, the cells were substantially aggregated, even after 7 days of incubation. In contrast, the cells attached and distributed on the HB-PEGDA/HA-SH/Gel-SH/CPC much better. After 7 days, the cell density was increased significantly. Likewisely, amino acid, RGD peptide, collagen and fibronectin were also introduced into the photonic hydrogel by us. All these results demonstrated that the photonic hydrogel showed a high chemical space for further functionalization and diverse specific moieties therefore can be introduced to enhance its function in an easy manner.

CONCLUSION

In this work, PEG hyperbranched polymers synthesized from *in-situ* RAFT polymerization with DS as the RAFT agent precursor was used for direct encapsulation of CPCs towards bio-optical applications. Compared to the counterpart prepared by the conventional RAFT technology, the HB-PEGDA synthesized by the *in-situ* RAFT technology get rid of undesired coloration, benefiting its optical uses. Importantly, the 3D HB-PEGDA contains high amount of pendent vinyl groups and can be crosslinked to form hydrogel quickly, offering a good protective effect to effectively maintain the structural integrity of the CPC films during pregel impregnation and gelation processes. The hydrogel-CPC composite showed credible and consistent coloration under diverse complex solution and

temperature conditions. Moreover, the hydrogel-CPC composite exhibits a good biocompatibility and it can be further functionalized easily to introduce specific functional moieties, such as the CAMs. In view of the easy-to-implement protocol, robust optical performance, excellent biocompatiblity together with the facile modification, we believe this novel type of structured photonic hydrogel will show great potential in bio-optical areas.

EXPERIMENTAL SECTION

Materials and reagents

Poly(ethylene glycol) diacrylate (PEGDA, average M_n = 700 g·mol^{-1}), 2, 2'-azobis(2-methylpronitrile) (AIBN), tetraethylthiuramdisulphide (DS), gelatin, acrylamide, N,N'-methylenebis(acrylamide) (BIS), 2-hydroxy-4'-(2-hydroxyethoxy)-2-methylpropiophenone (DEAP), butanone, diethyl ether and hexane were purchased from Sigma-Aldrich and used as received. Dulbecco's Modified Eagle's Medium (DMEM), fetal bovine serum (FBS), and penicillin/streptomycin were purchased from Invitrogen. Thiolated hyaluronic acid (HA-SH, Glycosil®, ESI BIO) was purchased from BioTime Inc. SiO_2 nanoparticles were synthesized according to a published method.[58] Water used in all experiments was purified using a Milli-Q Plus 185 water purification system (Millipore, Bedford, MA) with resistivity higher than 18 MW·cm.

Polymer synthesis and characterization

HB-PEGDA was synthesized by homopolymerization of PEGDA through the *in-situ* RAFT approach. Briefly, the PEGDA monomer (180 mmol, 25 *equiv.*) was firstly dissolved in butanone (450 mL) at a monomer concentration of 0.4 mol·L^{-1} in a two-neck flask. Then, the initiator (AIBN 10.08 mmol, 1.4 *equiv.*) and chain transfer agent (CTA, DS 7.2 mmol, 1 *equiv.*) were added into the flask. The mixture was bubbled with argon for 30 minutes. The oil bath was pre-heated to 70 °C. The polymerization was then performed at 70 °C. The polymerizationwas monitored by an Agilent 1260 Infinity GPC system equipped with a refractive index detector, a viscometer detector, and a dual-angle light-scattering detector (LS 15° and LS 90°). GPC columns (PolarGel-M, 7.5 mm × 300 mm; two in series) were eluted with DMF and 0.1% LiBr at a flow rate of 1 mL/min at 60 °C. GPC columns were calibrated with linear poly(methyl methacrylate) standards. To measure the molecular weight and monomer conversion, GPC samples were taken at different time points. Briefly, 50 μL of reaction mixture was taken and then diluted with 1 mL of DMF, filtered through a 0.45 μm filter, and them measured with GPC. To stop the polymerization, the flask was quenched with ice water and exposed to air. The polymers were purified by precipitation with hexane/diethyl ether solution (1:2 v/v) three times and then dried in vacuum oven for 48 hours to remove the residual solvent. Molecular weights and polydispersity index ($Đ$, M_w/M_n) of the final polymers products were determined by GPC. To confirm the hyperbranched structures, Mark-Houwink plot alpha values (α) of the polymers were determined. To this end, 10 mg of polymer products were dissolved in 2 mL of DMF, filtered through a 0.45 μm filter, and then measured by the GPC and the α values were calculated from triple detector. Chemical composition and purity of the polymers were determined with NMR (Bruker, 400 MHz), polymers were dissolved in $CDCl_3$, the chemical shifts were referenced to the lock $CDCl_3$. UV-*vis* spectra of the polymers dissolved in deionized water (10 mg/mL) were recorded using the SpectraMax® M3 Multi-Mode Microplate Reader.

Fabrication of HB-PEGDA/HA-SH hydrogel and rheological measurements

HB-PEGDA/HA-SH hydrogels were fabricated as follows: firstly, HB-PEGDA were dissolved in PBS buffers to a concentration of 2%, 4%, 6% or 8% (w/v), respectively. The commercially available HA-SH was diluted with PBS to a concentration of 1% (w/v) and its pH value was adjusted to 7.4 using 1 M NaOH solution. Then, the two solutions are mixed together with equal volumes (50 μL each) by vortex for 5 seconds. Afterwards, the mixture was transferred onto a parallel sample plate (diameter: 8 mm) for rheological measurements with a Discovery HR-2 Rheometer (TA Instruments). For a real-time crosslinking rheological study, an oscillatory time sweep was performed at 20 and 37 °C, respectively.

Construction of hydrogel-CPC composites and optical spectra measurement

The CPC film was prepared through a modified inward-growing self-assembly method.[59] Briefly, 150 μL colloidal suspension (solid content 2 wt%, SiO_2 nanoparticle diameter 209 nm) was dropped onto a glass substrate and then moved to an oven to complete the crystallization at 25 °C with a relative humidity of 70%. Hydrogel-CPC composites were constructed by directly pipeting the aforementioned HB-PEGDA/HA-SH mixture solution (100 μL in volume) onto the CPC surface. Reflectance peaks of the CPC film were recorded by an optical microscope equipped with a fibre optic spectrometer (Ocean Optics, USB 4000) and all spectra were taken perpendicular to the (1 1 1) crystal planes (the sample surfaces).

Cytotoxicity test of the hydrogel-CPC composites

The Swiss albino mouse embryo tissue cell line 3T3, human cervical cancer cell line HeLa were purchased from the American Type Culture Collection (ATCC). They were cultured in Dulbecco's modified Eagle Medium (DMEM) containing 10% FBS and 1% Penicillin/Streptomycin (P/S) at 37 °C, 5% CO_2, in a humid incubator under standard cell culture techniques. To evaluate the cytotoxicity of the HB-PEGDA polymer, the cells were seeded in 96 well-plate at a density of 8,000 cells/well in 100 μL medium. 24 hours later, the medium was replaced with 100 μL HB-PEGDA containing medium. The final concentration of the HB-PEGDA polymer in the medium was 50, 100, 250, 500 or 1000 mg·mL^{-1}, respectively. After incubation for another 24 hours, the cell viability was measured using LIVE/DEAD assays following the standard protocols. All the experiments were repeated at least four times.

To measure the cytotoxicity of the HB-PEGDA/HA-SH hydrogel-CPC composites, 3T3 or Hela cell suspension, HB-PEGDA, and HA-SH were mixed together and

dropped onto the CPC surface, the final cell concentration was 1 x 10^6 mL^{-1}. The composites were then transferred into a 24-well plate and 1 mL full cell medium was added into each well. The cell culture medium was changed every day. LIVE/DEAD assays were employed to visualize the living and dead cells at day 1, 3 and 7, respectively following the standard protocols. All the experiments were repeated at least four times.

Cell attachment study of the HB-PEGDA/HA-SH/Gel-SH hydrogel-CPC composites

To fabricate the HB-PEGDA/HA-SH/Gel-SH hydrogel-CPC composites, in a 1.5 mL Eppendorf tube, 200 μL HB-PEGDA (8%, w/v), 100 μL HA-SH (4%, w/v) and 100 μL Gel-SH (4%, w/v) DMEM solutions were mixed simultaneously by vortex for 5 seconds, and then transferred onto the CPC surface in a 48 well-plate and kept undisturbed at room temperature to form the hydrogels by crosslinking. 30 minutes later, 200 μL of stably GFP expressing HeLa cell suspension (20,000 cells in total) were added on the top of the hydrogel-CPC composite gently and kept undisturbed for another hour. The plate was then transferred to the cell incubator slowly to make sure the cells were not detached. The cells were incubated following standard cell culture protocols for 7 days and the cell culture medium was changed at day 2, day 4 and day 6. The cells were observed and GFP images of the cells were taken at day 1, day 3 and day 7, respectively using a fluorescent microscope (Olympus IX81). The HB-PEGDA/HA-SH hydrogel-CPC composites were prepared with the same polymer and crosslinker concentrations and used as the control. All the experiments were repeated at least four times.

ASSOCIATED CONTENT

Supporting Information.

The Supporting Information is available free of charge via the Internet at http://pubs.acs.org.

Chemical structure of HA-SH; additional characterization of the HB-PEGDA polymers from different polymerization time; NMR spectra of the HB PEGDA; real photo of the hydrogel-CPC composite; SEM images and reflectance spectra of the CPCs before and after hydrogel impregnation; rheological measurements of the as-obtained hydrogel-CPC composites.

AUTHOR INFORMATION

Corresponding Author

dezhong.zhou@ucd.ie (D.Z.);
wenxin.wang@ucd.ie (W.W.)

Author Contributions

J.Z. and H.Y. contributed equally to this work.

Notes

The authors declare no competing financial interest.

ACKNOWLEDGMENT

This work was supported by Science Foundation Ireland Principal Investigator Award (13/IA/1962), Investigator Award (12/IP/1688), Health Research Board of Ireland (HRA-POR-2013-412), Irish Research Council and H2020 Marie Skłodowska-Curie Actions Funding (CLNE/2017/358), National Natural Science Foundation of China (No. 51573129 and No. 51473117), National Natural Science Foundation of Jiangsu Province (BK20171013) and National Natural Science Funds for Distinguished Young Scholar (No. 51325305). Jing Zhang and Haiyang Yong contributed equally to this work.

REFERENCES

(1) Wang, X. R. ; Hu, J. M. ; Zhang, G. Y.; Liu, S. Y. Highly selective fluorogenic multianalyte biosensors constructed via enzyme-catalyzed coupling and aggregation-induced emission. *J. Am. Chem. Soc.* **2014**, 136, 9890-9893.

(2) Li, Z.; Fang, M.; LaGasse, M. K.; Askim, J. R.; Suslick, K. S. Colorimetric Recognition of Aldehydes and Ketones. *Angew. Chem. Int. Ed*. **2017**, 56, 9860–9863.

(3) Hou, J.; Zhang, H.; Yang, Q.; Li, M.; Jiang, L.; Song, Y. Hydrophilic – hydrophobic patterned molecularly imprinted photonic crystal sensors for high-sensitive colorimetric detection of tetracycline. *small* **2015**, 11, 2738-2742.

(4) Culver, H. R.; Clegg, J. R.; Peppas, N. A. Analyte-Responsive Hydrogels: Intelligent Materials for Biosensing and Drug Delivery, *Acc. Chem. Res.* **2017**, 50, 170–178.

(5) Chen, L.; Wang, X.; Lu, W.; Wu, X.; Li, J. Molecular imprinting: perspectives and applications, *Chem. Soc. Rev.* **2016**, 45, 2137–2211.

(6) Tsai, T.; Shen, S.; Cheng, C.; Chen, C. Paper-based tuberculosis diagnostic devices with colorimetric gold nanoparticles. *Sci. Technol. Adv. Mater.* 2013, **14**, 044404.

(7) Lee, S.; Barin, G.; Ackerman, C. M.; Muchenditsi, A.; Xu, J.; Reimer, J. A.; Lutsenko, S.; Long, J. R.; Chang, C. J. Copper Capture in a Thioether-Functionalized Porous Polymer Applied to the Detection of Wilson's Disease. *J. Am. Chem. Soc.* **2016**, 138, 7603–7609.

(8) Bridgeman, D.; Corral, J.; Quach, A.; Xian, X.; Forzani, E. Colorimetric humidity sensor based on liquid composite materials for the monitoring of food and pharmaceuticals. *Langmuir* **2014**, 30, 10785–10791.

(9) Lu, W.; Zhang, M.; Liu, K.; Fan, B.; Xia, Z.; Jiang, L. A fluoride-selective colorimetric and fluorescent chemosensor and its use for the design of molecular-scale logic devices. *Sens. Actuators. B Chem.* **2011**, 160, 1005–1010.

(10) Nam, J. M.; Jang, K. J.; Groves, J. T. Detection of proteins using a colorimetric bio-barcode assay. *Nat. Protoc.* **2007**, 2, 1438.

(11) Xia, F.; Zuo, X.; Yang, R.; Xiao, Y.; Kang, D.; Vallée-Bélisle, A.; Gong, X.; Yuen, J. D.; Hsu, B. B. Y.; Heeger, A. J.; Plaxco, K. W. Colorimetric detection of DNA, small molecules, proteins, and ions using unmodified gold nanoparticles and conjugated polyelectrolytes. *Proc. Natl. Acad. Sci. U.S.A.*, **2010**, 107, 10837–10841.

(12) Hong, Y.; Lam, J. W. Y.; Tang, B. Aggregation-induced emission: phenomenon, mechanism and applications. *Chem. Commun.* **2009**, 0, 4332–4353.

(13) Lei Z.; Yang, Y. A Concise Colorimetric and Fluorimetric Probe for Sarin Related Threats Designed via the "Covalent-Assembly" Approach. *J. Am. Chem. Soc.* **2014**, 136, 6594–6597.

(14) Wei, H.; Chen, C.; Han, B.; Wang, E. Enzyme colorimetric assay using unmodified silver nanoparticles. *Anal. Chem.* **2008**, 80, 7051–7055.

(15) Li, J.; Zhang, Z.; Xu, S.; Chen, L.; Zhou, N.; Xiong, H.; Peng, H. Label-free colorimetric detection of trace cholesterol based on molecularly imprinted photonic hydrogels. J. Mater. Chem. 2011, 21, 19267–19274.

(16) Yang, Q.; Peng, H.; Li, J.; Li, Y.; Xiong, H.; Chen, L. Label-free colorimetric detection of tetracycline using analyte-

responsive inverse-opal hydrogels based on molecular imprinting technology. New J. Chem. 2017, 41, 10174–10180.

(17) Zhang, Z.; Wang, H.; Chen, Z.; Wang, X.; Choo, J.; Chen, L. Plasmonic colorimetric sensors based on etching and growth of noble metal nanoparticles: Strategies and applications, Biosens Bioelectron. 2018, 114, 52–65.

(18) Shang, L.; Gu, Z.; Zhao, Y. Structural color materials in evolution. *Mater. Today*. **2016**, 19, 420–421.

(19) B. H. King, A. Gramada, J. R. Link, M. J. Sailor, Internally referenced ammonia sensor based on an electrochemically prepared porous SiO2 photonic crystal. *Adv. Mater.* **2007**, 19, 4044–4048.

(20) Yu, Z.; Wang, C. F.; Ling, L.; Chen, L.; Chen, S. Triphase microfluidic-directed self-assembly: anisotropic colloidal photonic crystal supraparticles and multicolor patterns made easy. *Angew. Chem. Int. Ed.* **2015**, 51, 2375–2378.

(21) Fu, F.; Shang, L.; Zheng, F.; Chen, Z.; Wang, H.; Wang, J.; Gu, Z.; Zhao, Y. Cells cultured on core-shell photonic crystal barcodes for drug screening. *ACS Appl. Mater. Interfaces*. **2016**, 8, 13840–13848.

(22) Zhang, L.; Xiong, Z.; Shan, L.; Zheng, L.; Wei, T.; Yan, Q. Layer-by-layer approach to (2+1)D photonic crystal superlattice with enhanced crystalline integrity. *small* **2015**, 11, 4910–4921.

(23) Riedrich-MÃuller, J.; Arend, C.; Pauly, C.; MÃijcklich, F.; Fischer, M.; Gsell, S.; Schreck, M.; Becher, C. Deterministic Coupling of a Single Silicon-Vacancy Color Center to a Photonic Crystal Cavity in Diamond. *Nano. Lett.* **2014**, 14, 5281–5287.

(24) Campbell, M.; Sharp, D. N.; Harrison, M. T.; Denning, R. G.; Turberfield, A. J. Fabrication of photonic crystals for the visible spectrum by holographic lithography. *Nature* **2000**, 404, 53–56.

(25) Zhang, J.; Tian, Y.; Ji, W.; Zhu, Z.; Wang, C.; Chen, S. Ultrasensitive responsive photonic crystal films derived from the assembly between similarly charged colloids and substrates towards trace electrolyte sensing. *J. Mater.Chem. C*. **2016**, 4, 6750–6755.

(26) Xu, H.; Cao, K. D.; Ding, H.; Zhong, Q.; Gu, H.; Xie, Z.; Zhao, Y.; Gu, Z. Spherical porphyrin sensor array based on encoded colloidal crystal beads for VOC vapor detection. *ACS Appl. Mater. Interfaces*. **2012**, 4, 6752–6757.

(27) Kuang, M.; Wang, J.; Bao, B.; Li, F.; Wang, L.; Jiang, L.; Song, Y. Inkjet Printing Patterned Photonic Crystal Domes for Wide Viewing-Angle Displays by Controlling the Sliding Three Phase Contact Line. *Adv. Optical Mater.* **2014**, 2, 34–38.

(28) Liu, S.; Wang, C.; Wang, X.; Zhang, J.; Tian, Y.; Yin, S.; Chen, S. Tunable Janus colloidal photonic crystal supraballs with dual photonic band gaps. *J. Mater. Chem. C*. **2014**, 2, 9431–9438.

(29) Kong, B.; Seog, J. H.; Graham, L. M.; Lee, S. B. Experimental considerations on the cytotoxicity of nanoparticles. *Nanomedicine (Lond).* **2011**, 6, 929–941.

(30) Ben-Moshe, M.; Alexeev, V. L.; Asher, S. A. Fast responsive crystalline colloidal array photonic crystal glucose sensors. *Anal. Chem.* **2006**, 78, 5149–5157.

(31) Yang, D. P.; Ye, S. Y.; Ge, J. P. Solvent wrapped metastable colloidal crystals: highly mutable colloidal assemblies sensitive to weak external disturbance. *J. Am. Chem. Soc.* **2013**, 135, 18370–18376.

(32) Hong, W.; Hu, X.; Zhao, B.; Zhang, F.; Zhang, D. Tunable photonic polyelectrolyte colorimetric sensing for anions, cations and zwitterions. *Adv. Mater.* **2010**, 22, 5043–5047.

(33) Fu, F.; Shang, L.; Chen, Z.; Yu, Y.; Zhao, Y. Bioinspired living structural color hydrogels. *Sci. Robot.* **2018**, 3, eaar8580.

(34) Shin, J.; Braun, P. V.; Lee, W. Fast response photonic crystal pH sensor based on templated photo-polymerized hydrogel inverse opal. *Sens Actuators B Chem.* **2010**, 150, 183–190.

(35) Lee, K.; Asher, S. A. Photonic crystal chemical sensors: pH and ionic strength. *J. Am. Chem. Soc.*, **2000**, 122, 9534–9537.

(36) Gur, D.; Palmer, B. A.; Leshem, B.; Oron, D.; Fratzl, P.; Weiner, S.; Addadi, L. The mechanism of color change in the neon tetra fish: a light-induced tunable photonic crystal array. *Angew. Chem. Int. Ed.* **2015,** 54, 12426–12430.

(37) Kang, J. H.; Kim, S. H.; Fernandez-Nieves, A.; Reichmanis, E. Amplified photon upconversion by photonic shell of cholesteric ciquid crystals. *J. Am. Chem. Soc.* **2017**, 139, 5708–5711.

(38) Fang, Y.; Ni, Y.; Leo, S. Y.; Taylor, C.; Basile, V.; Jiang, P. Reconfigurable photonic crystals enabled by pressure-responsive shape-memory polymers. *Nat. Commun.* **2015**, 6, 7416.

(39) Miao, Y.; Liu, B.; Zhang, K.; Liu, Y.; Zhang, H. Temperature tunability of photonic crystal fiber filled with Fe3O4 nanoparticle fluid. *Appl. Phys. Lett.* **2011**, 98, 021103.

(40) Ge, J.; Yin, Y. Responsive photonic crystals. *Angew. Chem. Int. Ed.* **2011**, 50, 1492–1522.

(41) Caminade, A. M.; Yan, D.; Smith, D. K. Dendrimers and hyperbranched polymers. *Chem. Soc. Rev.* **2015**, 44, 3870-3873.

(42) Jiang, W.; Zhou, Y.; Yan, D. Hyperbranched polymer vesicles: from self-assembly, characterization, mechanisms, and properties to applications. *Chem. Soc. Rev.* 2015, **44**, 3874–3889.

(43) Wang, D.; Zhao, T.; Zhu, X.; Yan, D.; Wang, W. Bioapplications of hyperbranched polymers. *Chem. Soc. Rev.* **2015**, 44, 4023–4071.

(44) Zhao, T.; Zheng, Y.; Poly, J.; Wang, W. Controlled multivinyl monomer homopolymerization through vinyl oligomer combination as a universal approach to hyperbranched architectures. *Nat. Commun.* **2013**, 4, 1873.

(45) Gao, Y.; Newland, B.; Zhou, D.; Matyjaszewski, K.; Wang, W. Controlled polymerization of multivinyl monomers: formation of cyclized/knotted single-chain polymer architectures. *Angew. Chem. Int. Ed.* **2017**, 56, 450–460.

(46) Zhao, T.; Zhang, H.; Newland, B.; Aied, A.; Zhou, D.; Wang, W. Significance of branching for transfection: synthesis of highly branched degradable functional poly (dimethylaminoethyl methacrylate) by vinyl oligomer combination. *Angew. Chem. Int. Ed.* **2014**, 53, 6095–6100.

(47) McMahon, S.; Kennedy, R.; Duffy, P.; Vasquez, J. M.; Wall, J. G.; Tai, H.; Wang, W. Poly (ethylene glycol)-based hyperbranched polymer from RAFT and its application as a silver-sulfadiazine-loaded antibacterial hydrogel in wound care. *ACS Appl. Mater. Interfaces*. **2016**, 8, 26648–26656.

(48) Zhou, D.; Cutlar, L.; Gao, Y.; Wang, W.; O'Keeffe-Ahern, J.; McMahon, S.; Duarte, B.; Larcher, F.; Rodriguez, B. J.; Greiser, U.; Wang, W. The transition from linear to highly branched poly (β -amino ester)s: Branching matters for gene delivery. *Sci. Adv.* **2016**, 2, e1600102.

(49) Tai, H.; Mather, M. L.; Howard, D.; Wang, W.; White, L. J.; Crowe, J. A.; Morgan, S. P.; Chandra, A.; Williams, D. J.; Howdle, S. M.; Shakesheff, K. M. Control of pore size and structure of tissue engineering scaffolds produced by supercritical fluid processing. *Eur. Cells. Mater.* **2007**, 14, 64–77.

(50) Xu, Q.; Guo, L.; A, S.; Gao, Y.; Zhou, D.; Greiser, U.; CreaghFlynn, J.; Zhang, H.; Dong, Y.; Cutlar, L.; Wang, F.; Liu, W.; Wang, W.; Wang, W. Injectable hyperbranched poly(β -amino ester) hydrogels with on-demand degradation profiles to match wound healing processes. *Chem. Sci.* **2018**, 9, 2179–2187.

(51) Zhou, D.; Gao, Y.; A, S.; Xu, Q.; Meng, Z.; Greiser, U.; Wang, W. Anticancer drug disulfiram for in situ RAFT polymerization: controlled polymerization, multifacet self-assembly, and efficient drug delivery. *ACS Macro Lett.* **2016**, 5, 1266–1272.

(52) Gao, Y.; Zhou, D.; Zhao, T.; Wei, X.; McMahon, S.; Ahern, J. O. K.; Wang, W.; Greiser, U.; Rodriguez, B. J.; Wang, W. Intramolecular cyclization dominating homopolymerization of multivinyl monomers toward single-chain cyclized/knotted polymeric nanoparticles. *Macromolecules* **2015**, 48, 6882–6889.

(53) Koh, M. L.; Konkolewicz, D.; Perrier, S. A simple route to functional highly branched structures: RAFT homopolymerization of divinylbenzene. *Macromolecules* **2011**, 44, 2715-2724.

(54) Nair, D. P.; Podgorski, M.; Chatani, S.; Gong, T.; Xi, W.; Fenoli, C. R.; Bowman, C. N. The thiol-Michael addition click reaction: a powerful and widely used tool in materials chemistry. *Chem. Mater.* **2014**, 26, 724–744.

(55) Drury, J. L.; Mooney, D. J. Hydrogels for tissue engineering: scaffold design variables and applications. *Biomaterials* **2003**, 24, 4337-4351.

(56) Xuan, R.; Wu, Q.; Yin, Y.; Ge, J. Magnetically assembled photonic crystal film for humidity sensing. *J. Mater. Chem.* **2011**, 21, 3672–3676.

(57) Zhang, H.; Dong, Y.; Wang, L.; Wang, G.; Wu, J.; Zheng, Y.; Yang, H.; Zhu, S. Low swelling hyperbranched poly (amine-ester) hydrogels for pH-modulated differential release of anticancer drugs. *J. Mater. Chem.* **2011**, 21, 13530–13537.

(58) Zhang, J.; Meng, Z.; Liu, J.; Schlaich, C.; Yu, Z.; Deng, X. Breath figure lithography for the construction of a hierarchical structure in sponges and their applications to oil/water separation. *J. Mater. Chem. A*. **2017**, 5, 16369–16375.

(59) Yan, Q.; Zhou, Z.; Zhao, X. S. Inward-growing self-assembly of colloidal crystal films on horizontal substrates. *Langmuir* **2005**, 21, 3158–3164.

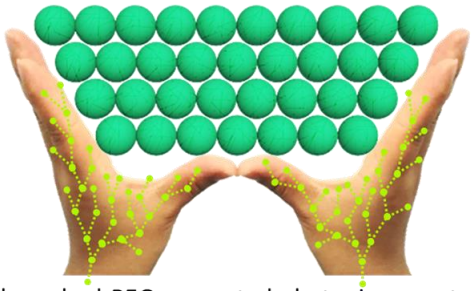

Hyperbranched PEG supported photonic nanostrucutures
for optical hydrogels

Table of Contents artwork